Title	Laser spectroscopy of NiBr: Ground and low-lying electronic states
Author(s)	Leung, JWH; Wang, X; Cheung, ASC
Citation	Journal Of Chemical Physics, 2002, v. 117 n. 8, p. 3694-3700
Issued Date	2002
URL	http://hdl.handle.net/10722/42042
Rights	Journal of Chemical Physics. Copyright © American Institute of Physics.

Laser spectroscopy of NiBr: Ground and low-lying electronic states

J. W-H. Leung, Xianghuai Wang, and A. S-C. Cheung[a)]
Department of Chemistry, The University of Hong Kong, Pokfulam Road, Hong Kong

(Received 2 April 2002; accepted 29 May 2002)

Four electronic states of NiBr have been studied using the technique of laser vaporization/reaction with supersonic cooling and laser induced fluorescence (LIF) spectroscopy. NiBr molecules were produced by reacting laser ablated nickel atoms and ethyl bromide (C_2H_5Br). High resolution LIF spectrum between 724 and 810 nm was recorded, which consists of the (2,0), (1,0), and (0,0) bands of the [13.2] $^2\Pi_{3/2}$–$X\,^2\Pi_{3/2}$ system and the [13.2] $^2\Pi_{3/2}$–$A\,^2\Delta_{5/2}$ system, and also the (v,0) with $v=0-4$ bands of the [12.6] $^2\Sigma^+$–$X\,^2\Pi_{3/2}$ system. Spectra of four isotopic molecules: $^{58}Ni^{79}Br$, $^{58}Ni^{81}Br$, $^{60}Ni^{79}Br$, and $^{60}Ni^{81}Br$ were observed and analyzed. Least squares fit of rotationally resolved transition lines yielded accurate molecular constants for the $X\,^2\Pi_{3/2}$, $A\,^2\Delta_{5/2}$, [12.6] $^2\Sigma^+$, and [13.2] $^2\Pi_{3/2}$ electronic states of NiBr. The bond length, r_0, measured for the $X\,^2\Pi_{3/2}$ and $A\,^2\Delta_{5/2}$ states is 2.196 28 and 2.164 45 Å, respectively. A molecular orbital diagram has been constructed to explain the four observed electronic states. This work represents the first high-resolution spectroscopic study of NiBr. © *2002 American Institute of Physics.*
[DOI: 10.1063/1.1494777]

I. INTRODUCTION

Spectroscopic studies of transition metal diatomic halides have been an active research area in the past few decades.[1–5] The importance of these halides ranges from catalysis,[6] surface science,[7] to astrophysics. Astrophysically, because of high cosmic abundance of transition metal elements in stars, it is likely that some of these halide molecules may exist in significant amount in astrophysical sources.[4,5] Furthermore, diatomic halides are simple model systems that can provide insights into the role of the *d* orbitals in chemical bonds.[2] The effects of the halogens as a ligand to split the transition metal *d* orbitals can be studied when halides of the same transition metal are compared. Spectroscopic investigation of the halides not only yield accurated molecular properties such as bond length, bond strength, and dipole moment, etc.; it also gives information on the occupation of specific molecular orbitals formed from the transition metal and the halogen atom. Due primarily to the near degeneracy of the *d* orbitals, electronic states are generally close lying, and also with many unpaired electrons that give rise to high spin multiplicity states, spectrum of transition metal halides is usually complicated. Furthermore, transition metal and halogen atoms very often have isotopes with appreciable abundance, which give rise to isotopic spectra in the same vicinity causing heavy spectral overlap. Therefore, electronic spectrum of such a seemingly simple diatomic molecule could be complex and congested. High-resolution spectroscopic techniques are usually necessary for detailed study of this class of molecules.[8]

Among the first transition metal period, there have been considerable interests recently in the spectroscopic properties of nickel fluoride[9–13] and nickel chloride.[14–19] Work includes study of the ground and excited electronic states using high resolution Fourier transform spectroscopy, laser spectroscopy, and microwave spectroscopy. Fundamental understanding of the electronic structure of the ground and excited states of these two halide molecules begins to emerge. However, for the latter two diatomic halides, only very limited knowledge is available for NiBr and nothing at present is known for NiI. For NiBr, low-resolution emission spectra in the region 3800–5000 Å have been photographed by Reddy *et al.*[20,21] Six band systems have been identified of which three are single-headed bands and the other three are double-headed bands. Darji *et al.*[22] reported some new measurements of bands in the spectral region 4000–4500 Å. Gopal *et al.*[23,24] investigated the thermal emission spectrum of NiBr produced by heating a mixture of nickel powder and nickel bromide in a vacuum graphite furnace. Eight subsystems were detected, with three attributed to transitions from a $^2\Delta$ ground state. Only vibrational constants were reported. None of the earlier work was able to resolve the complex rotational structure of NiBr.

In this paper, we report rotationally resolved near-infrared spectroscopic study of electronic transition of low-lying states of NiBr using the technique of laser vaporization/reaction with supersonic cooling and laser induced fluorescence (LIF) spectroscopy. Three electronic transitions have been identified, namely [13.2] $^2\Pi_{3/2}$–$X\,^2\Pi_{3/2}$, [13.2] $^2\Pi_{3/2}$–$A\,^2\Delta_{5/2}$, and [12.6] $^2\Sigma^+$–$X\,^2\Pi_{3/2}$ systems. {For the upper state whose characterization is less completed, we follow Clinton *et al.* [J. Mol. Spectrosc. **102**, 441 (1983)] to use the square bracket empirical notations.} Spectra of four isotopic species: $^{58}Ni^{79}Br$, $^{58}Ni^{81}Br$, $^{60}Ni^{79}Br$, and $^{60}Ni^{81}Br$ were observed and analyzed. Line positions of all the measured transitions of individual isotopic molecules were fit to retrieve vibrational and rotational constants for [13.2] $^2\Pi_{3/2}$, [12.6] $^2\Sigma^+$, $A\,^2\Delta_{5/2}$, and $X\,^2\Pi_{3/2}$ states.

a)Author to whom correspondence should be addressed. Tel: (852) 2859 2155; Fax: (852) 2857 1586; electronic mail: hrsccsc@hku.hk

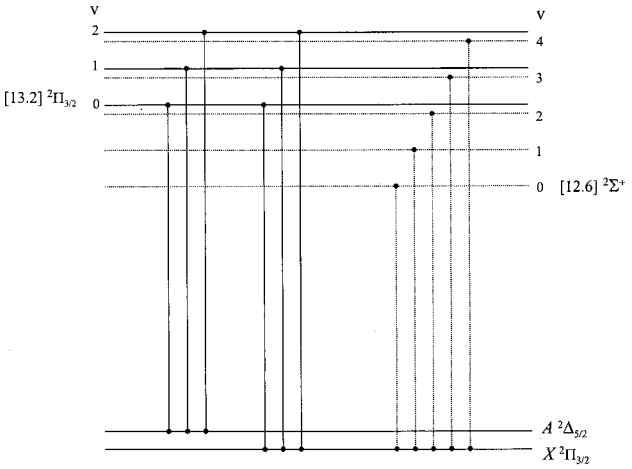

FIG. 1. Vibronic transitions observed and analyzed in this work.

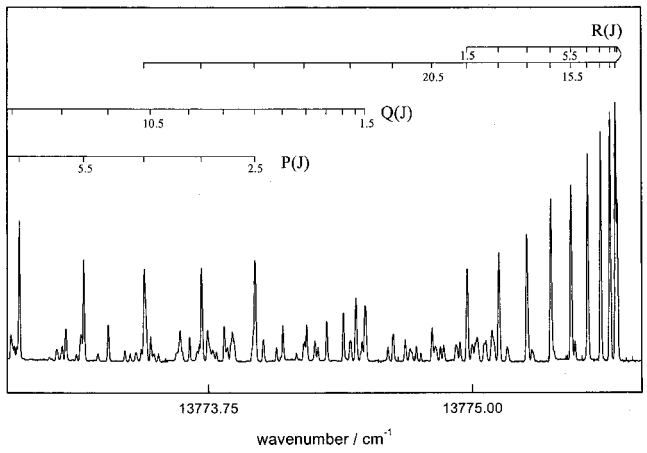

FIG. 2. The (2,0) band of the [13.2] $^2\Pi_{3/2}$–$X\ ^2\Pi_{3/2}$ transition of NiBr.

II. EXPERIMENTAL DETAILS

The laser vaporization/reaction free jet expansion laser induced fluorescence spectrometer employed in this work has been described previously.[25,26] Only a brief description of the experimental conditions is given here. A pulse of 532 nm, 9–10 mJ, and 10 ns from a Nd:YAG laser was focused on the surface of a nickel metal rod to generate nickel atoms in plasma. A pulsed valve, with an appropriate delay, released gas mixtures of 2% C_2H_5Br in argon into the reaction region. NiBr molecules were produced by the reaction of Ni atoms with C_2H_5Br in the gas phase. The operating cycle of the Nd:YAG laser-valve system was 10 Hz. Jet-cooled NiBr molecules were excited by a cw ring Ti:sapphire laser pumped by an argon ion laser. Laser induced fluorescence signal was collected by means of a lens system and detected by a photomultiplier tube (PMT). The PMT signal was fed into a boxcar integrator for averaging. A wavemeter with an accuracy of 1 part in 10^7 was used to measure the wavelength of the Ti:sapphire laser. The accuracy of the wavemeter has been calibrated using I_2 lines in the near infrared region.[27] The absolute accuracy of transition line positions measured in this work was about 0.002 cm^{-1}. The electronic transition spectrum of NiBr was obtained by connecting a few hundred scans using the wavemeter reading.

The new near infrared bands observed were readily attributed to NiBr based on their vibrational intervals, and, more importantly, the four dominating isotopic species: $^{58}Ni^{79}Br$, $^{58}Ni^{81}Br$, $^{60}Ni^{79}Br$, and $^{60}Ni^{81}Br$. The linewidth of the molecular transition is about 0.006 cm^{-1} (200 MHz).

III. RESULTS AND DISCUSSION

A. General feature

The laser induced fluorescence spectrum of NiBr in the near infrared region between 724 and 810 nm has been observed and analyzed. The band structure is generally complex due to the appearance of the four isotopic species and small B values (0.097 cm^{-1}) for both the excited and ground states. Two of the three electronic transition systems identified, namely, [13.2] $^2\Pi_{3/2}$–$X\ ^2\Pi_{3/2}$ and [13.2] $^2\Pi_{3/2}$–$A\ ^2\Delta_{5/2}$ were easily recognized and analysis. However, the [12.6] $^2\Sigma^+$–$X\ ^2\Pi_{3/2}$ system was difficult to confirm because

TABLE I. Molecular constants for the [13.2] $^2\Pi_{3/2}$, $A\ ^2\Delta_{5/2}$, and $X\ ^2\Pi_{3/2}$ states of NiBr (cm^{-1}).

State	Parameter	$^{58}Ni^{79}Br$	$^{58}Ni^{81}Br$	$^{60}Ni^{79}Br$	$^{60}Ni^{81}Br$
[13.2] $^2\Pi_{3/2}$	T_2	13774.5296(2)	13771.5866(2)	13769.0850(3)	13766.1126(2)
	B	0.095898(3)	0.094898(2)	0.094057(4)	0.093051(4)
	10^8D	7.62(8)	7.42(7)	7.4(2)	7.1(1)
	T_1	13485.2129(2)	13483.7670(2)	13482.5247(3)	13481.0643(3)
	B	0.096312(3)	0.095307(3)	0.094457(4)	0.093443(4)
	10^8D	7.9(1)	7.7(1)	7.6(2)	7.5(2)
	T_0	13194.0691(2)	13194.1391(2)	13194.1716(3)	13194.2425(3)
	B	0.096730(3)	0.095716(3)	0.094861(4)	0.093841(4)
	10^8D	8.1(1)	7.95(9)	7.8(1)	7.7(1)
$A\ ^2\Delta_{5/2}$	T_0	37.4666(2)	37.4573(2)	37.4438(3)	37.4335(3)
	B	0.107705(3)	0.106562(3)	0.105599(4)	0.104453(4)
	10^7D	1.38(2)	1.355(8)	1.32(1)	1.29(1)
$X\ ^2\Pi_{3/2}$	T_0	0.00	0.00	0.00	0.00
	B	0.104599(3)	0.103520(4)	0.102608(2)	0.101529(2)
	10^8D	4.365[a]	4.278[a]	4.201[a]	4.110[a]

[a]Indicate the values are fixed in the least squares fit. Errors in parentheses are one standard deviation in units of the last significant figure quoted.

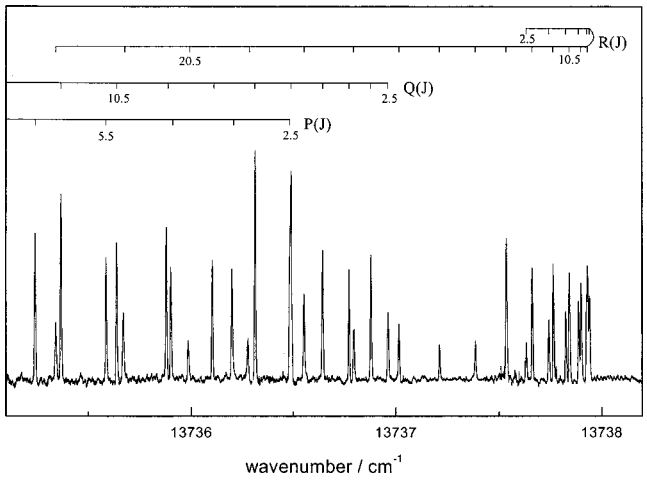

FIG. 3. The (2,0) band of the [13.2] $^2\Pi_{3/2}$–$A\,^2\Delta_{5/2}$ transition of NiBr.

branches from the [13.2] $^2\Pi_{3/2}$–$A\,^2\Delta_{5/2}$ transition overlapped in the same region. Figure 1 depicts the eleven transition bands studied in this work.

B. [13.2] $^2\Pi_{3/2}$–$X\,^2\Pi_{3/2}$ system

Strong *R* heads near 13 775.7, 13 486.4, and 13 195.4 can readily be identified, based on their vibrational intervals they are assigned, respectively, as the 2–0, 1–0, 0–0 bands of a new electronic transition. Each of these bands consists of resolved *P*, *Q*, and *R* branches. Line assignments were relatively simple because the origin lines of each branch were observed. Figure 2 shows the band head region of the (2,0) band. Because of the difference between the vibrational constants of the upper and lower levels, the (2,0) band of the ^{58}Ni^{79}Br is slightly shifted away from bands of other isotopes. We still have problems in assigning the weaker features in Fig. 2. The lowest observed *J* numbering for *P*, *Q*, and *R* branches are 2.5, 1.5, and 1.5, respectively, which allows the establishment of the $\Omega''=\Omega'=3/2$ component for both states. Furthermore, the *P* and *R* branches are much stronger than the *Q* branch which is consistent with a $\Delta\Lambda=0$ transition. The observed bands are the (2,0), (1,0), and

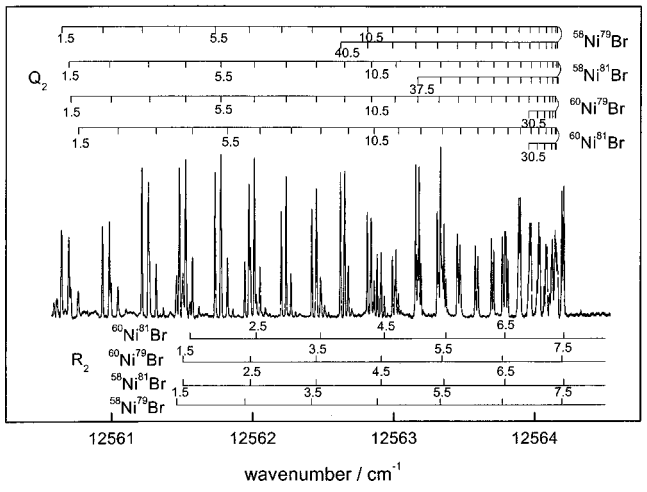

FIG. 4. The (0,0) band of the [12.6] $^2\Sigma^+$–$X\,^2\Pi_{3/2}$ transition of NiBr.

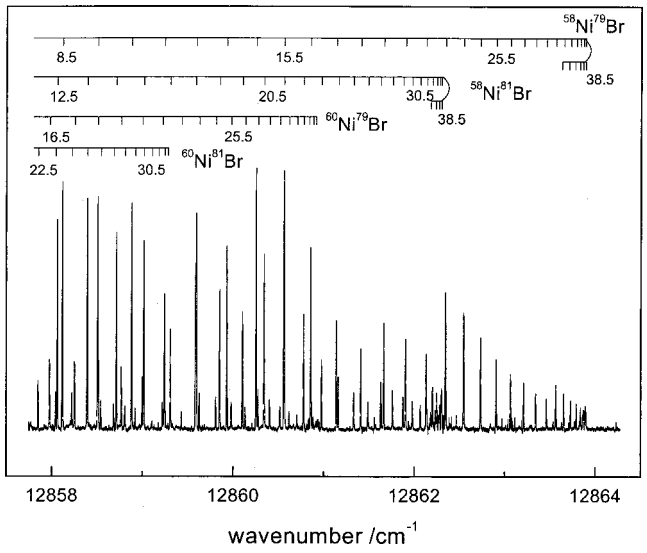

FIG. 5. The heads of the R_2 branches of the (1,0) band of the [12.6] $^2\Sigma^+$–$X\,^2\Pi_{3/2}$ transition of NiBr.

(0,0) bands of the [13.2] $^2\Pi_{3/2}$–$X\,^2\Pi_{3/2}$ transition. Since our spectrum was recorded at relatively low temperature, only low *J* lines were observed ($J\leqslant 29.5$), and no Λ-doubling was detected. The observed line positions were fit to a standard formula,[28]

$$\nu = T_0 + B'J'(J'+1) - D'[J'(J'+1)]^2 - \{B''J''(J''+1) - D''[J''(J''+1)]^2\}. \quad (1)$$

In our analysis, we first performed a band-by-band least squares fit to the line positions and subsequently all the available line positions of an each individual isotope were merged in the final fit. The results are listed in Table I.

C. [13.2] $^2\Pi_{3/2}$–$A\,^2\Delta_{5/2}$ system

Strong band heads occur at 13 738.0, 13 448.6, and 13 157.6 cm^{-1} which are again readily assigned as the 2–0, 1–0, and 0–0 band of a new electronic transition system. Figure 3 shows a portion of the (2, 0) band of this system. The first line of each *P*, *Q*, and *R* branches are with $J=2.5$, which indicates that the $\Omega''=2.5$ and $\Omega'=1.5$ of the lower and upper electronic states, respectively. It can be easily seen that the *P* and *Q* branches are stronger than the *R* branch which agrees well with a $\Delta\Lambda=-1$ transition. The observed bands are the (2, 0), (1, 0), and (0, 0) band of the [13.2] $^2\Pi_{3/2}$–$A\,^2\Delta_{5/2}$ transition. Similar to the earlier discussed $^2\Pi_{3/2}$–$^2\Pi_{3/2}$ transition, the line positions of these bands were fit to the formula in Eq. (1). After an individual band of this transition was fitted, we notice that the rotational constants of the upper state agree well with those obtained in the [13.2] $^2\Pi_{3/2}$–$X\,^2\Pi_{3/2}$ system. A merged least squares fit of the line positions of [13.2] $^2\Pi_{3/2}$–$X\,^2\Pi_{3/2}$ and the [13.2] $^2\Pi_{3/2}$–$A\,^2\Delta_{5/2}$ transitions determines accurately the separation between the $A\,^2\Delta_{5/2}$ and $X\,^2\Pi_{3/2}$ states, which is 37.466 cm^{-1}. The results are also listed in Table I.

TABLE II. Molecular constants for the $[12.6]\ ^2\Sigma^+$ state of NiBr (cm^{-1}). Errors in parentheses are one standard deviation in units of the last significant figure quoted.

Parameter	$^{58}Ni^{79}Br$	$^{58}Ni^{81}Br$	$^{60}Ni^{79}Br$	$^{60}Ni^{81}Br$
T_4	13723.4127(2)	13717.4696(2)	13712.4422(2)	13706.4389(2)
B	0.096682(2)	0.095683(2)	0.094836(2)	0.093844(2)
10^8D	9.50(5)	9.35(3)	9.15(8)	8.86(6)
γ	−0.43549(2)	−0.43101(1)	−0.42739(2)	−0.42290(3)
T_3	13435.1714(2)	13430.7023(2)	13426.9138(2)	13422.4003(2)
B	0.097112(2)	0.096106(2)	0.095254(2)	0.094252(2)
10^8D	9.61(9)	9.41(4)	9.22(5)	9.01(5)
γ	−0.43820(1)	−0.43367(1)	−0.42992(2)	−0.42540(2)
T_2	13145.1497(2)	13142.1719(2)	13139.6380(2)	13136.6309(2)
B	0.097540(2)	0.096528(2)	0.095670(2)	0.094663(2)
10^8D	9.65(4)	9.46(3)	9.25(3)	9.07(3)
γ	−0.44095(1)	−0.43637(1)	−0.43258(1)	−0.42795(2)
T_1	12853.3502(2)	12851.8830(2)	12850.6187(2)	12849.1373(2)
B	0.097971(2)	0.096950(2)	0.096088(2)	0.095071(2)
10^8D	9.70(2)	9.50(2)	9.32(2)	9.12(4)
γ	−0.44369(2)	−0.43913(1)	−0.43525(2)	−0.43066(2)
T_0	12559.7773(2)	12559.8377(2)	12559.8591(2)	12559.9213(2)
B	0.098392(2)	0.097367(2)	0.096498(2)	0.095475(2)
10^8D	9.78(4)	9.54(3)	9.48(6)	9.33(6)
γ	−0.44642(2)	−0.44180(1)	−0.43789(2)	−0.43325(2)

D. $[12.6]\ ^2\Sigma^+ - X\ ^2\Pi_{3/2}$ system

Among these three systems, the $[12.6]\ ^2\Sigma^+ - X\ ^2\Pi_{3/2}$ system was the most difficult to assign. Because this band involves a transition between a $^2\Sigma^+$ in case (b) and a $^2\Pi$ state in case (a), which has six strong branches, namely, P_2, Q_2, R_2, P_{12}, Q_{12}, and R_{12}. Besides, owing to small B values of both states and the presence of four isotopic molecules with comparable abundance, these six branches overlap heavily in the same spectral region. In order to assign these branches, a program was written which used estimated B and γ values for the upper state, and the B value of the $X\ ^2\Pi_{3/2}$ state to predict the transition lines of these six branches. Figure 4 shows a portion of the Q_2 and R_2 branches of the (0, 0) band. For this band, the branches of the four isotopic molecules have origins lie very close to each other. It can be noticed quickly that the R_2 branches are running parallel to each other and form heads at the higher energy side. In addition, the (0, 0) band consists of two strong P_2 and Q_2 band heads at 12 560.4 and 12 564.2 cm^{-1}, respectively. The first line of all six branches were identified and assigned. Figure 5 depicts the R_2 head region of the (1, 0) band. Due to a shift in band origin of the isotopic species, the R_2 head of each isotopic is nicely spread. Five vibronic transitions have been observed and assign as $(v,0)$ bands with $v=0-4$ (see Fig. 1). The observed line positions were fit to:

Upper state $^2\Sigma^+$ term values,

$$F_1'(J)=B(J'-0.5)(J'+0.5)+D[(J'-0.5)(J'+0.5)]^2+\tfrac{1}{2}\gamma(J'-0.5) \quad (2)$$

and

$$F_2'(J)=B(J'+0.5)(J'+1.5)-D[(J'+0.5)(J'+1.5)]^2-\tfrac{1}{2}\gamma(J'+1.5), \quad (3)$$

Lower state $X\ ^2\Pi_{3/2}$ term values,

$$F_2''(J)=T_0-B''J''(J''+1)-D''[J''(J''+1)]^2, \quad (4)$$

where γ is the spin-rotation constant. Transition line positions were calculated by subtracting the lower state term values from the upper state term values. Initially, we performed a band-by-band fit and then merged all line positions in a grand least squares fitting. The molecular constants for the

TABLE III. Equilibrium molecular constants for the $[12.6]\ ^2\Sigma^+$ and $[13.2]\ ^2\Pi_{3/2}$ states of NiBr (cm^{-1}). Errors in parentheses are one standard deviation in units of the last significant figure quoted.

State	Parameter	$^{58}Ni^{79}Br$	$^{58}Ni^{81}Br$	$^{60}Ni^{79}Br$	$^{60}Ni^{81}Br$
$[12.6]\ ^2\Sigma$	T_e	12412.323(2)	12413.154(2)	12413.824(2)	12414.664(3)
	ω_e	295.352(2)	293.806(2)	292.505(2)	290.944(2)
	$\omega_e x_e$	0.8886(4)	0.8796(4)	0.8718(4)	0.8628(5)
	B_e	0.098609(3)	0.097580(2)	0.096709(2)	0.095681(2)
	α_e	0.00043(9)	0.00042(6)	0.00042(8)	0.00041(7)
$[13.2]\ ^2\Pi_{3/2}$	T_e	13047.8120	13048.6470	13049.3228	13050.1665
	ω_e	292.971	291.4362	290.1459	288.5953
	$\omega_e x_e$	0.91355	0.90415	0.89640	0.88675
	B_e	0.096939	0.0959205	0.095063	0.09404
	α_e	0.000418	0.000409	0.000404	0.000398

TABLE IV. Observed and calculated isotopic displacements for NiBr (cm^{-1}).

		$^{58}Ni^{81}Br$		$^{60}Ni^{79}Br$		$^{60}Ni^{81}Br$	
State	V	$\Delta\nu_{obs}$	$\Delta\nu_{cal}$	$\Delta\nu_{obs}$	$\Delta\nu_{cal}$	$\Delta\nu_{obs}$	$\Delta\nu_{cal}$
$[12.6]\,^2\Sigma^+$	4	5.943	6.042	10.971	11.123	16.974	17.223
	3	4.469	4.559	8.258	8.393	12.771	12.997
	2	2.978	3.058	5.512	5.630	8.519	8.718
	1	1.467	1.538	2.732	2.832	4.213	4.385
	0	−0.060	0	−0.082	0	−0.144	0
$[13.2]\,^2\Pi_{3/2}$	2	2.943	3.032	5.445	5.582	8.417	8.644
	1	1.446	1.526	2.688	2.791	4.149	4.321
	0	−0.071	0	−0.102	0	−0.173	0

different bands are given in Table II. A list of 4650 line positions of all four isotopes for the (2, 0), (1, 0), and (0, 0) bands of both $[13.2]\ ^2\Pi_{3/2}-X\ ^2\Pi_{3/2}$ and $[13.2]\ ^2\Pi_{3/2}-A\ ^2\Delta_{5/2}$ systems, and (4, 0), (3, 0), (2, 0), (1, 0), and (0, 0) bands of the $[12.6]\ ^2\Sigma^+-X\ ^2\Pi_{3/2}$ system of NiBr is available from EPAPS.[29] The root-mean-squares (RMS) errors of the merged least squares fit is 0.0013 cm^{-1}. Molecular constants for the $X\ ^2\Pi_{3/2}$, $A\ ^2\Delta_{5/2}$, $[12.6]\ ^2\Sigma^+$, and $[13.2]\ ^2\Pi_{3/2}$ states are reported for the first time. Equilibrium molecular constants for $[12.6]\ ^2\Sigma^+$ and $[13.2]\ ^2\Pi_{3/2}$ states of all isotopes are given in Table III.

E. Isotopic shifts

Our vibrational quantum number assignment of the upper state can be further confirmed by examining the isotopic displacement from band origins of the four isotopes. Table IV compares the observed and calculated vibrational isotopic displacement, $\Delta\nu$. Molecular parameters of isotopic species are approximately related by various powers of the mass dependence $\rho=(\mu/\mu_i)^{1/2}$, where μ and μ_i are the reduced masses of $^{58}Ni^{79}Br$ and one of the isotopes, respectively.[28] Since $^{58}Ni^{79}Br$ is one of the most abundant isotope, isotopic effects are calculated relative to it. Table V shows a comparison of calculated and observed equilibrium molecular parameters. The agreement of these values is excellent. The isotopic shift for the (0, 0) band is negative indicates that the vibrational frequency in the upper state must be less than that of the ground state. Because of our experimental conditions, the molecules produced were quite cold only the lowest vibrational level, $v=0$, of the $X\ ^2\Pi_{3/2}$ and $A\ ^2\Delta_{5/2}$ were populated, and no vibrational constants of the $X\ ^2\Pi_{3/2}$ and $A\ ^2\Delta_{5/2}$ states could be determined.

F. Molecular constants for the $X\ ^2\Pi_{3/2}$, $A\ ^2\Delta_{5/2}$, $[12.6]\ ^2\Sigma^+$, and $[13.2]\ ^2\Pi_{3/2}$ states

Yamazaki *et al.*[30] studied the microwave spectrum of two isotopes of NiBr and obtained preliminary rotational constants for the $v=0$ level of the $A\ ^2\Delta_{5/2}$ state. The following is a comparison of these values (cm^{-1}):

Parameter	This work		Yamazaki *et al.*[30]	
	$^{58}Ni^{79}Br$	$^{58}Ni^{81}Br$	$^{58}Ni^{79}Br$	$^{58}Ni^{81}Br$
B	0.107705	0.106562	0.107663	0.106560
10^7D	1.38	1.36	1.111	1.075

The agreement of the B values between our determinations and those of Yamazaki *et al.*[30] is excellent. However, our D values are larger, this may be because only relatively low J lines ($J<39$) were measured in this work our precision on these constants are slightly lower. We have attempted to fit our data fixing the D constant at the Yamazaki *et al.*[30] value, but the RMS errors jumped to 0.0018 cm^{-1} much larger than our 0.0013 cm^{-1}. In addition, in our least squares fitting, it was performed with the B and D terms, but Yamazaki *et al.*[30] used higher order terms including B, D, and H. From the observed rotational constants, the bond length, r_0, obtained is 2.196 28 and 2.164 45 Å, for the $X\ ^2\Pi_{3/2}$ and $A\ ^2\Delta_{5/2}$ states, respectively, and the equilibrium bond length, r_e, for the $[12.6]\ ^2\Sigma^+$ and $[13.2]\ ^2\Pi_{3/2}$ states is, respectively, 2.2621 and 2.3502 Å. We note in passing that the γ value for the $[12.6]\ ^2\Sigma^+$ is relatively large and negative. This indicates that there are nearby $^2\Pi$ states making contributions through second-order interactions to the γ parameter. It has been shown by Simard *et al.*[31] that the negative value of γ in a $^2\Sigma^+$ state could result from the interac-

TABLE V. Mass-scaled parameters of NiBr.

		Observed			Calculated		
State	Isotope	ω_e	$\omega_e x_e$	B_e	ω_e	$\omega_e x_e$	B_e
$[12.6]\ ^2\Sigma^+$	$^{58}Ni^{81}Br$	293.806	0.8796	0.097580	293.804	0.8793	0.097578
	$^{60}Ni^{79}Br$	292.505	0.8718	0.096709	292.503	0.8715	0.096715
	$^{60}Ni^{81}Br$	290.944	0.8628	0.095681	290.940	0.8623	0.095650
$[13.2]\ ^2\Pi_{3/2}$	$^{58}Ni^{81}Br$	291.436	0.9042	0.095920	291.436	0.9040	0.095926
	$^{60}Ni^{79}Br$	290.146	0.8964	0.095063	290.145	0.8960	0.095077
	$^{60}Ni^{81}Br$	288.595	0.8868	0.094040	288.595	0.8865	0.094064

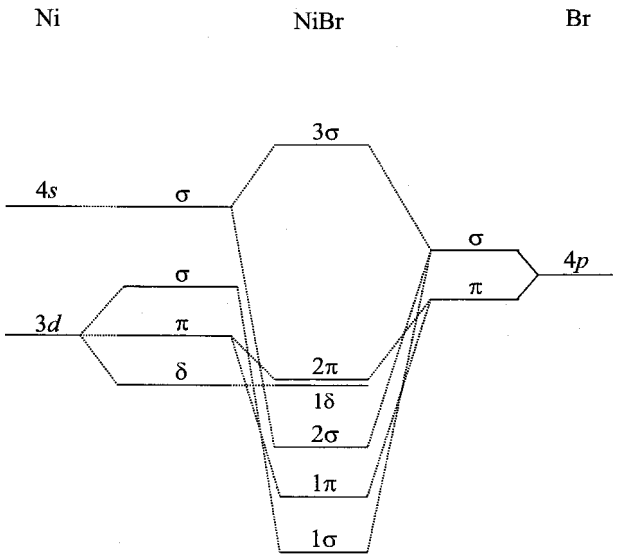

FIG. 6. Molecular orbital energy level diagram of NiBr.

tion between the $^2\Sigma^+$ and a $^2\Pi$ state arising from an electronic configuration with π^3 such as reaction (5) below.

G. Electronic configurations

The electronic states in NiBr are similar to those found in the isovalent molecules: NiF (Ref. 32) and NiCl,[15] which have the same number of valence electrons. The electronic configurations giving rise to the observed states are

$$(2\sigma)^2(1\delta)^4(2\pi)^3 \quad X\,^2\Pi_i, \tag{5}$$

$$(2\sigma)^2(1\delta)^3(2\pi)^4 \quad A\,^2\Delta_i, \tag{6}$$

$$(2\sigma)^1(1\delta)^4(2\pi)^4 \quad ^2\Sigma^+. \tag{7}$$

Figure 6 shows the molecular orbital (MO) formed from the Ni metal $4s$ and $3d$ atomic orbitals (AO) and bromine $4p$ AOs. The 1δ MO is almost entirely a Ni $3d\delta$ AO because there are no other orbitals of δ symmetry lying nearby. The 2π MO is a Ni-based slight antibonding combination of Ni $3d\pi-4p\pi$ and of the bromine $4p\pi$ AOs. The above mentioned electronic states can be easily understood from this MO diagram. We have also examined another electronic configuration, which may give rise to electronic excited states,

$$(2\sigma)^2(1\delta)^3(2\pi)^3(3\sigma)^1 \quad ^2\Pi_i(2),\ ^4\Pi_i,\ ^2\Phi_i,\ ^4\Phi_i. \tag{8}$$

The [13.2] $^2\Pi_{3/2}-X\,^2\Pi_{3/2}$ transition observed in this work corresponds to the promotion of an electron from the 1δ orbital to the antibonding 3σ orbital. The [13.2] $^2\Pi_{3/2}-A\,^2\Delta_{5/2}$ transition corresponds to promoting an electron from the 2π to the 3σ orbital. The [12.6] $^2\Sigma^+-X\,^2\Pi_{3/2}$ transition system is likely to be the promotion of an electron from the 2σ orbital to the 2π orbital. It is easily noticed that the smaller B values of the $X\,^2\Pi_{3/2}$ is consistent with the occupation of the slightly antibonding 2π orbital.

It would be useful to examine the known ground and low-lying electronic states of NiF, NiCl, and NiBr to understand the effects of the halogen as a ligand to split the d orbitals of the Ni atom. In the construction of the molecular orbital diagram two aspects should be considered: First, the relative energy of the $3d$ and $4s$ orbital of the Ni and the p orbital of the halogen atoms. Since the first ionization potential of an atom is the smallest amount of energy necessary to remove an electron, it corresponds, therefore, to the energy of losing the outermost subshell electron.[33] The ionization potential (IP) of the halogen atoms down the group: F, Cl, Br, and I is, respectively, 17.42, 12.97, 11.81, and 10.45 eV, but for Ni the IP is only 7.64 eV. This indicates that, in a molecular orbital diagram, the p orbitals of the halogen atoms down the group must be moving closer and closer to the $3d$ and $4s$ orbitals of the Ni atom. Secondly, it is expected that the electron distribution of these metal halides depends upon electron affinity of the atoms. The halogen atoms have larger electronegativity and would be able to attract electron distribution closer to it; therefore, nickel halides are basically ionic. The order of halogen ions in the spectrochemical series is $F^->Cl^->Br^->I^-$, which implies that the separation between the molecular orbitals $3d\sigma$, $3d\pi$, and $3d\delta$ from the metal $3d$ will be strongly halogen dependent and with the fluoride giving the largest separation.[34] It would be interesting to note the energy of the $A\,^2\Delta_{5/2}$ state with respect to the $X\,^2\Pi_{3/2}$ is 1095,[32] 158,[14] and 37 cm^{-1}, respectively, for NiF, NiCl, and NiBr, which drops drastically from NiF to NiBr. Since the $A\,^2\Delta_{5/2}$ state arises from $(2\sigma)^2(1\delta)^3(2\pi)^4$, where the 1δ MO should have the least influence from the halogens because 1δ MO is mainly from the nickel atom and there is no other orbital of the same symmetry nearby to interact with it. The relative drop in energy of the $A\,^2\Delta_{5/2}$ state should be viewed as the changes that occur in the 2π and 2σ orbitals in the halides rather than the 1δ MO. These changes in 2π and 2σ can be ascribed to the change in the relative orbital energy of the $3d$ and $4s$ AO of Ni and the p AO of the halogens, and the drop in separation between the $3d\sigma$, $3d\pi$, and $3d\delta$ orbitals by the halogen as a ligand. With the observations in NiF, NiCl, and NiBr, it is reasonable to expect that the 1δ MO of the next member of the halides, namely NiI, would continue to drop and will give rise to a $^2\Delta_{5/2}$ state as the ground state. This is because iodine has an even smaller IP than Br and also is lower down in the spectrochemical series. We have work in progress to study the electronic spectra of NiI in our laboratory to confirm this.

ACKNOWLEDGMENTS

The authors would like to thank Dr. Emi Yamazaki for communicating to us the molecular constants of the $A\,^2\Delta_{5/2}$ state prior to publication and Ms. Jinghua Dai for her technical assistance. The work described here was supported by a grant from the Committee on Research and Conference Grants of the University of Hong Kong.

[1] K. P. Huber and G. Herzberg, *Constants of Diatomic Molecules* (van Nostrand, New York, 1979).
[2] C. W. Bauschlicher, Jr., S. P. Walch, and S. R. Langhoff, *Quantum Chemistry: The Challenge of Transition Metals and Chemistry*, NATO ASI Series C, edited by A. Veillard (Reidel Dordrecht, 1986).
[3] S. R. Langhoff and C. W. Bauschlicher, Jr., Annu. Rev. Phys. Chem. **39**, 181 (1988).
[4] E. Hirota, Annu. Rep. Prog. Chem., Sect. C: Phys. Chem. **96**, 95 (2000).

[5] P. F. Bernath, Annu. Rep. Prog. Chem., Sect. C: Phys. Chem. **96**, 177 (2000).
[6] C. N. R. Rao, Annu. Rev. Phys. Chem. **40**, 291 (1989).
[7] M. Wojuechowsba, J. Habu, S. Lomnicki, and J. Stoch, J. Mol. Catal. A: Chem. **141**, 155 (1999).
[8] W. Demtröder, *Laser Spectroscopy*, 2nd ed. (Springer-Verlag, Berlin, 1996).
[9] C. Dufour and B. Pinchemel, J. Mol. Spectrosc. **173**, 70 (1995).
[10] C. Focsa, C. Dufour, and B. Pinchemel, J. Mol. Spectrosc. **182**, 65 (1997).
[11] Yang Chen, Jin Jin, Changjin Hu, Xueliang Yang, Xingxiao Ma, and Congxiang Chen, J. Mol. Spectrosc. **203**, 37 (2000).
[12] Jin Jin, Yang Chen, Xueliang Yang, Qin Ran, and Congxiang Chen, J. Mol. Spectrosc. **208**, 18 (2001).
[13] Jin Jin, Qin Ran, Xueliang Yang, Yang Chen, and Congxiang Chen, J. Phys. Chem. A **105**, 11177 (2001).
[14] T. Hirao, C. Dufour, B. Pinchemel, and P. F. Bernath, J. Mol. Spectrosc. **202**, 53 (2000).
[15] A. Poclet, Y. Krouti, T. Hirao, B. Pinchemel, and P. F. Bernath, J. Mol. Spectrosc. **204**, 125 (2000).
[16] Y. Krouti, A. Poclet, T. Hirao, B. Pinchemel, and P. F. Bernath, J. Mol. Spectrosc. **210**, 41 (2001).
[17] E. Yamazaki, T. Okabayashi, and M. Tanimoto, Astrophys. J. Lett. **551**, L199 (2001).
[18] J. J. O'Brien, J. S. Miller, and L. C. O'Brien, J. Mol. Spectrosc. **211**, 93 (2002).
[19] L. C. O'Brien, K. M. Homann, T. L. Kellerman, and J. J. O'Brien, J. Mol. Spectrosc. (in press).
[20] S. P. Reedy and P. T. Ro, Proc. Phys. Soc. **75**, 275 (1960).
[21] S. P. Reedy, N. Narayana, and P. T. Rao, Opt. Pura Apl. **20**, 69 (1987).
[22] A. B. Darji and N. R. Shah, Curr. Sci. **48**, 349 (1979).
[23] R. Gopal and M. M. Joshi, Curr. Sci. **50**, 1061 (1981).
[24] R. Gopal and M. M. Joshi, Indian J. Phys., B **59**, 309 (1985).
[25] Q. Ran, W. S. Tam, C. Ma, and A. S-C. Cheung, J. Mol. Spectrosc. **198**, 175 (1999).
[26] Q. Shi, Q. Ran, W. S. Tam, J. W-H. Leung, and A. S-C. Cheung, Chem. Phys. Lett. **339**, 154 (2001).
[27] S. Gerstenkorn, J. Verges, J. Chevillard, *Atlas des Spectres d'Absorption de la Molecule d'Iode*, 11000–14000 cm^{-1} (Presses der CNRS, Paris, 1982).
[28] G. Herzberg, *Spectra of Diatomic Molecules* (Van Nostrand, New York, 1950).
[29] See EPAPS Document No. E-JCPSA6-117-003232 for the observed line positions of the (2,0), (1,0) and (0,0) bands of both [13.2] $^2\Pi_{3/2}$–$X\ ^2\Pi_{3/2}$ and [13.2] $^2\Pi_{3/2}$–$A\ ^2\Delta_{5/2}$ systems, and (4,0), (3,0), (2,0), (1,0), and (0,0) bands of the [12.6] $^2\Sigma^+$–$X\ ^2\Pi_{3/2}$ system of NiBr. This document may be retrieved via the EPAPS homepage (http://www.aip.org/pubservs/epaps.html) or from ftp.aip.org in the directory /epaps/. See the EPAPS homepage for more information.
[30] Emi Yamazaki (private communication, 2001).
[31] B. Simard, J. K. G. Watson, A. J. Merer, and T. C. Steimle, J. Chem. Phys. **111**, 6148 (1999).
[32] P. Carette, C. Dufour, and B. Pinchemel, J. Mol. Spectrosc. **161**, 323 (1993).
[33] Y. Jean, F. Volatron, and J. Burdett, *An Introduction to Molecular Orbitals* (Oxford University Press, Oxford, 1993).
[34] T. M. Dunn, *Physical Chemistry: An Advanced Treatise*, edited by H. Eyring and H. Jost (Academic, New York, 1970), Vol. V, Chap. 5.